THE JOURNAL OF PHYSICAL CHEMISTRY B

Article

pubs.acs.org/JPCB

Solvent-Free Dynamic Nuclear Polarization of Amorphous and Crystalline *ortho*-Terphenyl

Ta-Chung Ong,[†,‡] Melody L. Mak-Jurkauskas,[§] Joseph J. Walish,[‡,∥] Vladimir K. Michaelis,[†,‡] Björn Corzilius,[†,‡] Albert A. Smith,[†,‡] Andrew M. Clausen,[§] Janet C. Cheetham,[§] Timothy M. Swager,[‡] and Robert G. Griffin*[,†,‡]

[†]Francis Bitter Magnet Laboratory, Massachusetts Institute of Technology, Cambridge, Massachusetts 02139, United States

[‡]Department of Chemistry, Massachusetts Institute of Technology, Cambridge, Massachusetts 02139, United States

[§]Amgen Inc., 360 Binney Street, Cambridge, Massachusetts 02142, United States

[∥]DyNuPol Inc., Newton, Massachusetts 02458, United States

Supporting Information

ABSTRACT: Dynamic nuclear polarization (DNP) of amorphous and crystalline *ortho*-terphenyl (OTP) in the absence of glass forming agents is presented in order to gauge the feasibility of applying DNP to pharmaceutical solid-state nuclear magnetic resonance experiments and to study the effect of intermolecular structure, or lack thereof, on the DNP enhancement. By way of $^{1}H-^{13}C$ cross-polarization, we obtained a DNP enhancement (ε) of 58 for 95% deuterated OTP in the amorphous state using the biradical bis-TEMPO terephthalate (bTtereph) and ε of 36 in the crystalline state. Measurements of the ^{1}H T_1 and electron paramagnetic resonance experiments showed the crystallization process led to phase separation of the polarization agent, creating an inhomogeneous distribution of radicals within the sample. Consequently, the effective radical concentration was decreased in the bulk OTP phase, and long-range $^{1}H-^{1}H$ spin diffusion was the main polarization propagation mechanism. Preliminary DNP experiments with the glass-forming anti-inflammation drug, indomethacin, showed promising results, and further studies are underway to prepare DNP samples using pharmaceutical techniques.

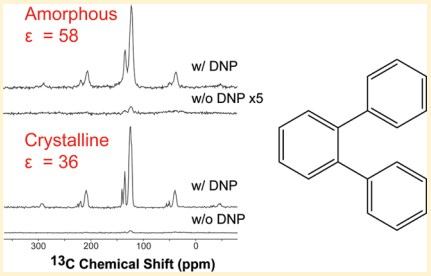

INTRODUCTION

Solid-state properties of active pharmaceutical ingredients (APIs) and drug formulations directly impact the safety and efficacy of a drug.[1−3] For example, a drug that is poorly soluble as a crystal oftentimes is more soluble if it can be prepared in an amorphous form, increasing its bioavailability. Solid-state nuclear magnetic resonance (NMR) is a uniquely informative and versatile analytical technique in pharmaceutical research that includes analysis of the final solid form of the drug, quantification of amorphous content, excipient interactions, and salt and polymorph screening. In practice, solid-state NMR is performed alongside other analytical techniques such as electron microscopy, X-ray diffraction, IR and Raman spectroscopies, differential scanning calorimetry (DSC), and thermogravimetric analysis (TGA) to produce a complete characterization of the API and its formulation. Compared to other techniques, solid-state NMR has the advantage of being an inherently quantitative method that nondestructively interrogates the whole sample. Depending on the system of interest, it can be used, for example, to identify and quantify polymorphs, detect the number of molecules in a unit cell, and elucidate the presence of a hydrate and/or solvate, investigate structural and dynamic properties over a wide range of time scales, monitor stability against degradation over time, and analyze crystalline and amorphous environments.[4,5]

Although informative, NMR is intrinsically an insensitive analytical technique as a result of the inherently low nuclear spin polarization. This problem can be further compounded by low natural abundance NMR active nuclei (e.g., ^{13}C, ^{15}N, ^{17}O, etc.). These challenges cause drug formulation screening by solid-state NMR to be a time-consuming process. Dynamic nuclear polarization (DNP) at cryogenic temperatures has been shown to provide significant enhancements for NMR signals. The gains in sensitivity afforded by DNP are typically one to two orders-of-magnitude and reduce the need for lengthy signal-averaging thereby dramatically reducing the data acquisition time.[6−14] As a result, DNP has found utility in NMR applied to membrane proteins,[15,16] amyloid fibrils,[17] inorganic complexes,[18] silicon surface functional groups,[19] metabolomics,[20] and medical magnetic resonance imaging (MRI).[21,22] Extension of microwave-driven DNP to analyze APIs and pharmaceutical formulations will potentially lead to significant savings in cost and time.

Currently, most DNP samples are prepared in a glass-forming medium such as glycerol/water or DMSO/water, which functions as a cryoprotectant to protect biological

Received: November 13, 2012
Revised: February 18, 2013
Published: February 19, 2013

   dx.doi.org/10.1021/jp311237d | *J. Phys. Chem. B* 2013, 117, 3040−3046

samples (e.g., proteins) against freezing damage.[23,24] In addition, the glassy matrix serves to uniformly disperse the mono- or biradical polarization agents that optimize the DNP enhancement.[25−27] However, dissolving APIs or their solid formulations in glassing media eliminates the solid-state structure under investigation and is unsuitable for studying pharmaceuticals. Previously, Vitzthum et al. conducted DNP experiments on an amorphous powder mixture of a decapeptide (DP) containing a spin-labeled decapeptide (DP*) without using solvent. The study obtained a DNP enhancement (ε) of up to 4, and an overall enhancement (ε_{global}) of up to 10 by taking into account factors such as Boltzmann population difference at cryogenic temperatures, faster nuclear relaxation, and nuclear spin bleaching caused by close proximity to paramagnets.[28] In a separate study, Lilly Thankamony et al. examined solvent-free DNP using mesoporous silica functionalized with TEMPO moieties and obtained an enhancement of 3 from direct ^{29}Si polarization.[29]

In contrast to previous experiments, the research direction described here ultimately aims to prepare solvent-free samples for DNP using common pharmaceutical sample preparation techniques that create dispersed radical polarization agents (e.g., TEMPO based radicals, BDPA, trityl, etc.) within the sample. To pursue this goal and to more thoroughly understand the DNP process, a solvent-free matrix that displays both amorphous and crystalline states is required. Importantly, our approach results in a rare direct comparison between identical amorphous and crystalline systems using DNP-NMR.

We present herein a comparison of signal enhancements employing DNP for the glass-former *ortho*-terphenyl (OTP) in its amorphous (i.e., glassy) and crystalline states. OTP is a well-studied organic glass forming solid[30] consisting of a central benzene ring with two pendant phenyl rings attached in positions ortho to one another. Steric effects produce an out-of-plane twisting of the pendant phenyls and allow the molecule to exist as a viscous supercooled-liquid for an extended period of time upon cooling from the melt.[31] Rapid freeze-quenching of the molten OTP creates a glass with a glass transition temperature (T_g) of −30 °C. At room temperature, supercooled liquids crystallize in a matter of minutes, as shown in Figure 1. The phase behavior of OTP allows for the manipulation of its physical state *in situ* during the DNP-NMR experiment (i.e., permitting us to observe both the crystalline- and amorphous-state DNP enhancements for a given sample without unpacking the NMR rotor). In turn, this allows for direct comparison of DNP enhancements using the identical OTP sample and packing conditions.

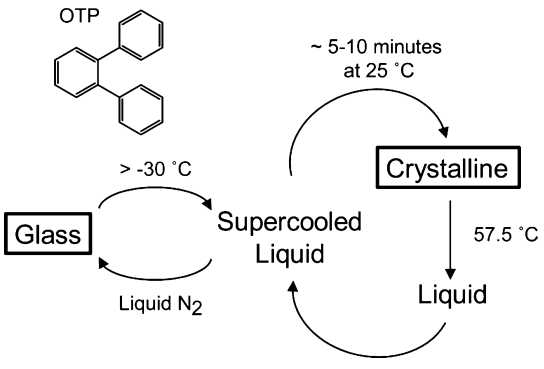

Figure 1. Phase transition scheme of *ortho*-terphenyl (OTP).

EXPERIMENTAL SECTION

Materials. *ortho*-Terphenyl (OTP, >99%) and 4-hydroxy-TEMPO (TEMPOL) were purchased from Sigma-Aldrich (St. Louis, MO) and used without further purification. d_{14}-OTP (98%) was purchased from Cambridge Isotope Laboratories, Inc. (Andover, MA). The hydrophobic biradical polarization agent bis-TEMPO terephthalate (bTtereph) was synthesized from TEMPOL and terephthaloyl chloride as described in the Supporting Information.

Sample Preparation. A radical polarization agent (TEMPOL or bTtereph) was incorporated into OTP at concentrations between 0.25 and 1 mol % by melting and mixing at elevated temperatures. The solution was then inserted into an NMR probe precooled to 80 K for rapid quenching bypassing the onset of crystallization and enabling the amorphous state measurements. The crystalline sample was obtained by removing the amorphous sample from the precooled NMR probe and waiting until in situ crystallization occurred under ambient conditions and was checked visually through the transparent sapphire NMR rotor.

DNP NMR. All Dynamic Nuclear Polarization Enhanced Nuclear Magnetic Resonance (DNP NMR) experiments were conducted on a custom-built 212 MHz (5 T, ^{1}H) spectrometer (courtesy of Dr. David Ruben, Francis Bitter Magnet Lab). The magnet is equipped with a superconducting sweep coil with a range of ±0.05 T, and a field mapping unit for accurate field measurements. Continuous wave high power (>8 W) microwaves were generated by a custom-built 140 GHz gyrotron.[32] All experiments used a custom-designed cryogenic three-channel (^{1}H−^{13}C−^{15}N) MAS probe with a commercial 4 mm spinning module (Revolution NMR, Fort Collins, CO). The probe is equipped with a cryogenic sample eject system[33] to allow rapid exchange of samples, which is crucial for our in situ studies. All ^{13}C spectra were acquired with MAS frequency of 4.5 kHz and with two pulse phase modulation (TPPM)[34] proton decoupling. For the cross-polarization[35] experiments, the CP contact time, τ_{CP}, was 2.0 ms at ν_{rf} of 83 kHz. For the DNP enhanced spectra, the number of acquisitions was 32. For the unenhanced spectra, the number of acquisitions was 2000. For the amorphous samples, the recycling time between scans was 60 s. For the crystalline samples, the recycling time between scans was 240 s.

Electron Paramagnetic Resonance (EPR). Continuous-wave 9.7 GHz (X-Band) EPR spectra were recorded on a Bruker Elexsys E580 spectrometer using a dielectric ring resonator ER 4118X-MD5 operating in the TE_{011} mode. The measurement temperature of 80 K was reached inside an ER 4118CF-O flow cryostat using liquid nitrogen as a cryogen. The amorphous sample was prepared by flash freezing OTP supercooled liquid inside a 4 mm o.d. EPR tube in liquid nitrogen before insertion into the EPR probe. The crystalline sample was prepared by removing the amorphous sample from the EPR probe after respective measurements and letting it warm at ambient conditions until complete crystallization was confirmed by visual means after which it was reinserted into the probe.

RESULTS

In consideration of the fact that the ^{1}H concentration affects the polarization transfer and spin diffusion efficiency responsible for DNP enhancements,[36−39] a series of samples were prepared by incorporating 1 mol % TEMPOL monoradical into

dx.doi.org/10.1021/jp311237d | J. Phys. Chem. B 2013, 117, 3040−3046

OTP with the deuteration level ranging from 0% to 95%. The ^{13}C cross-polarization MAS DNP enhancement (ε) measurements from these samples are shown in Figure 2 for both

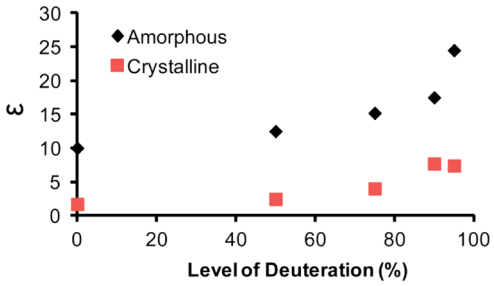

Figure 2. ^{13}C CPMAS DNP enhancement (ε) of OTP containing 1 mol % TEMPOL as a function of levels of deuteration.

amorphous and crystalline OTP. Amorphous OTP was shown to have ε between 10 (100% ^{1}H) and 25 (5% ^{1}H), while crystalline OTP enhancements were between 1.7 and 7.7, respectively. For both amorphous and crystalline OTP, deuteration provided significant gains in enhancement consistent with past DNP studies.

Hu et al. have shown that ε is substantially larger using nitroxide-based biradicals as compared to TEMPO monoradicals when cross-effect is the dominant DNP mechanism.[40] The cross-effect mechanism involves a three-spin flip−flip−flop process between two electrons and a nucleus.[41−45] Biradicals are more efficient and produce larger enhancements than the equivalent monoradical electron concentration as a result of their larger $e^{-}-e^{-}$ dipolar couplings. TOTAPOL[46] is an established water-soluble biradical that is used in many DNP experiments; however, we found that this agent was not miscible with OTP, and a new biradical, bis-TEMPO terephalate (bTtereph, as shown in Figure 3), was synthesized

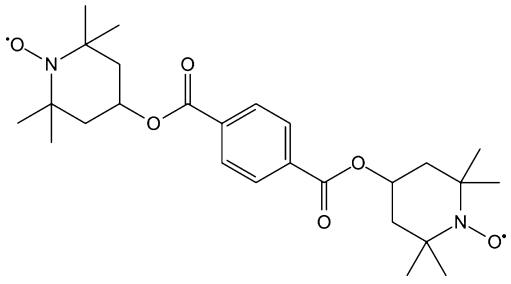

Figure 3. Structure of bis-TEMPO terephthalate (bTtereph).

for this experiment. Heating is required to melt OTP, and we conducted thermogravimetric analysis (TGA) and differential scanning calorimetry (DSC) of bTtereph to establish its thermal stability. The results (Figure S1, Supporting Information) indicated radical stability up to 160 °C, well above the melting point of OTP (57.5 °C); this enabled bTtereph to be mixed in warm OTP liquid (~60 °C) without fear of thermal degradation. The DNP analysis of these mixtures revealed that bTtereph provided a larger ε in OTP than the equivalent TEMPOL radical concentration. As shown in Figure 4, for 95% deuterated OTP with 0.5 mol % bTtereph, the ^{13}C CPMAS ε for the amorphous sample increased to 58, and in the crystalline sample, the ε increased to 36. DNP enhancements by direct ^{13}C polarization were also measured at the same external magnetic fields as the CPMAS ε measure-

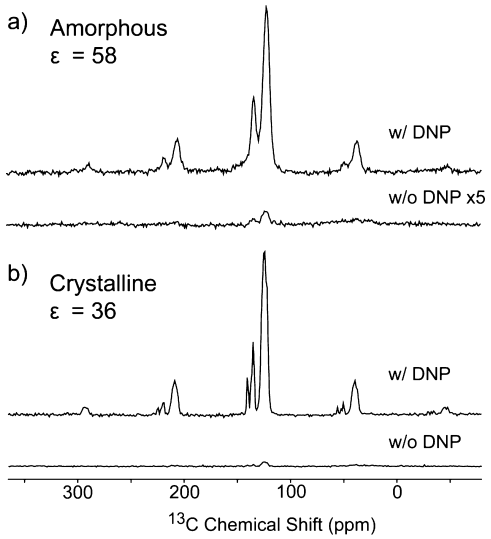

Figure 4. ^{13}C CPMAS DNP enhanced spectra of 95% deuterated OTP with 0.5 mol % bTtereph for the (a) amorphous and (b) crystalline states. The spectra are plotted with the DNP off spectra (no microwaves) to demonstrate the increase in signal-to-noise.

ments were conducted, and in these measurements, the ε in the amorphous state was 67 and the crystalline state was 50. We also determined the ^{13}C CPMAS ε for 100% protonated OTP with 0.5 mol % bTtereph to compare with the heavily deuterated sample and found enhancements of 35 and 3.3 in the amorphous and crystalline states, respectively.

A field-dependent enhancement profile was measured for bTtereph (Figure S2, Supporting Information) in 95% deuterated OTP, and the results were consistent with previously reported TOTAPOL[46] or bTbk[27] nitroxide-based radicals. We found that ε does not vary significantly with either increasing microwave power from 7 to 11 W or with bTtereph concentration ranging from 0.125 to 0.5 mol %, for both amorphous and crystalline states, as shown in Supporting Information, Figures S3 and S4, respectively.

^{1}H polarization buildup curves of the 95% deuterated amorphous and crystalline OTP with 0.25 mol % bTtereph were measured to determine the time required to reach signal saturation. The ^{1}H NMR signal for amorphous OTP reached its maximum very quickly with a buildup time constant (τ_B) of 8.3 s, as shown in Figure 5a. This result is consistent with past DNP samples prepared in glass forming solvents such as glycerol/water or DMSO/water.[46] For crystalline OTP, a dramatic increase in irradiation time was required to saturate the NMR signal, as shown in Figure 5b. Moreover, the ^{1}H buildup curve for the crystalline state exhibited a biphasic behavior, which can be described by eq 1:[47]

$$M(t) = M_{\infty}(1 - f\, e^{-t/\tau_{B1}} - (1 - f)\, e^{-t/\tau_{B2}}) \quad (1)$$

where buildup of bulk magnetization $M(t)$ is treated as the sum of two first order processes with time constants, τ_{B1} and τ_{B2}, and f denoting the fraction of the population polarized by the first process. Empirically fitting the data with eq 1 showed that the initial fast process had τ_{B1} of 22 s, and the slower polarization buildup that followed had τ_{B2} of 202 s, with 35% of the OTP polarized by the initial fast process. It was found that τ_{B1} is inversely related to radical concentration (i.e., a decrease in the ^{1}H build-up time constant occurred with increasing radical concentration). Conversely, τ_{B2} did not show significant

dx.doi.org/10.1021/jp311237d | J. Phys. Chem. B 2013, 117, 3040−3046

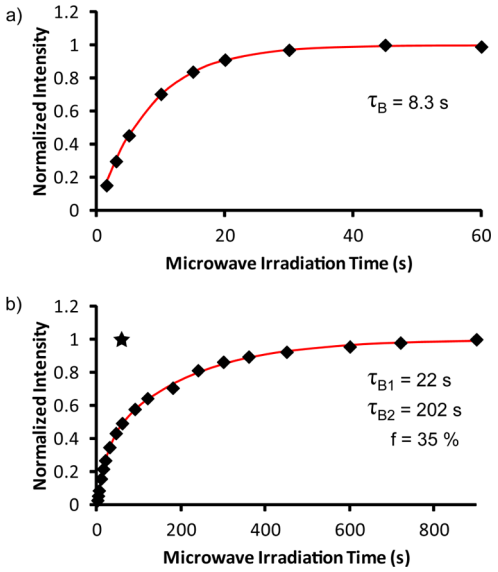

Figure 5. ^{1}H polarization buildup curves of (a) amorphous and (b) crystalline 95% deuterated OTP with 0.25 mol % bTtereph. The red line shows the exponential curve fitting of the data, with the amorphous data fitted with a monoexponential buildup equation, $M(t) = M_\infty(1 - e^{-t/\tau_B})$, and the crystalline data fitted with a biexponential buildup equation, $M(t) = M_\infty(1 - f\,e^{-t/\tau_{B1}} - (1 - f)\,e^{-t/\tau_{B2}})$. The star in panel b marks the amorphous saturation point obtained in panel a to demonstrate the substantial increase in signal saturation time observed for the crystalline sample.

dependence on the radical until high concentrations were reached. This suggests that the bTtereph radical phase separates into distinct domains during the crystallization of the OTP. Therefore, both a fast radical induced polarization buildup (^{1}H near the radical clusters) and a slow long-range ^{1}H−^{1}H dipolar coupling of spin-polarization contributed to the overall longer polarization buildup time observed for OTP crystals. Values of τ_{B1}, τ_{B2}, and f with respect to bTtereph concentration are reported in Table 1.

Table 1. Biphasic DNP ^{1}H Polarization Buildup Time Constants (τ_{B1} and τ_{B2}) and Fraction (f) of Crystallized OTP Polarized by the First, Fast Process at Various bTtereph Concentrations; the Errors Are Calculated Based on Biexponential Fitting

$\chi_{bTtereph}$ (mol %)	τ_{B1} (s)	τ_{B2} (s)	f (%)
0.125	39 ± 3.9	201 ± 20.3	43
0.25	22 ± 1.7	202 ± 10.9	35
0.5	16 ± 0.5	119 ± 6.8	57

Continuous-wave, 9 GHz EPR spectra of bTtereph in fully deuterated OTP were measured for both amorphous and crystalline states, as shown in Figure 6. Although the amorphous sample features a typical well-resolved EPR spectrum of a bis-nitroxide biradical, the spectrum of the crystalline sample is dominated by a featureless single line with a g-value similar to the average (isotropic) g-value of the nitroxide. Spectral simulations using the Easyspin package[48] (see Supporting Information for more details) show that the isotropic line has a Lorentzian shape and underlies a line width distribution with mean and variance of both ∼84 MHz (Figure S5, Supporting Information). We assume that this resonance arises from the bTtereph that phase-separates during

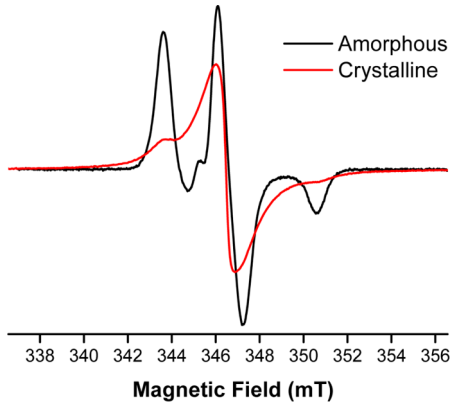

Figure 6. CW EPR field profile of bTtereph at 9.7 GHz in either amorphous or crystalline fully deuterated OTP. EPR amplitudes were corrected in order to achieve equal double integral values.

crystallization of the OTP with varying domain size. Strong electron−electron exchange couplings in these clusters lead to exchange-narrowed, homogeneous EPR lines. Additionally, a small contribution (∼7% of the overall signal intensity) can be attributed to isolated bTtereph molecules with spectral features equal to those obtained for the amorphous sample. This points either to a small amount of co-crystallization of bTtereph in OTP or to an incomplete crystallization process. These observations are further supported by pulsed EPR experiments at 9 and 140 GHz. While bTtereph in fully deuterated amorphous OTP allowed for echo detection of the EPR spectrum (see Figure S6, Supporting Information, for 140 GHz spectrum), we were unable to obtain echoes in the crystalline state, most probably due to ultrafast relaxation of phase-separated bTtereph.

DISCUSSION

DNP of Amorphous and Crystalline Solids. As observed from measurements of DNP enhancements, ^{1}H polarization buildup time, and EPR spectra, our results are largely in agreement with current literature that DNP is optimally performed in a glass or amorphous solid in which radical polarization agents are homogeneously dispersed. Figure 6 is a comparison of the EPR spectra of bTtereph in amorphous and crystalline fully deuterated OTP. The strong electron−electron coupling observed for the crystalline sample suggests that bTtereph appears to cluster in crystalline OTP, meaning that radical-rich and radical-poor regions are created during crystallization. The inhomogeneous radical distribution leads to smaller DNP enhancements and longer, biphasic ^{1}H polarization buildup times. This effect has been reported in other systems as well; Dementyev et al. observed a similar biphasic polarization buildup for DNP of partially crystalline silicon microparticles at 1.4 K.[49] The amorphous region of these silicon particles contains high concentration of paramagnetic impurities in the form of dangling bonds, while the crystalline region contains few such impurities. This creates an inhomogeneous distribution of radical polarization agents, and as a result, the nuclear relaxation time, T_1, becomes longer in the crystalline region compared to the amorphous region, leading to the biphasic polarization buildup that we also observed for OTP crystals.

Despite the disadvantage of radical clustering, we nevertheless observed that, by using biradicals as polarization agents and by deuteration, a significant DNP enhancement could still

dx.doi.org/10.1021/jp311237d | J. Phys. Chem. B 2013, 117, 3040−3046

be obtained for the crystalline system. Moreover, as shown in Figure 4, the linewidths were not significantly affected by the presence of biradicals, meaning that DNP can provide large enhancements in dry, solvent-free crystalline systems, while maintaining excellent spectral resolution. In light of the lowered enhancement due to radical clustering, we note that a low ^{1}H concentration, in this case by ~90−95% deuteration, is absolutely crucial by way of $^{1}H-^{13}C$ cross-polarization. We observed that 95% deuterated crystalline OTP with 0.5 mol % bTtereph yields ε of 36, while the ε decreases to 3.3 in a sample that is 100% protonated. This finding underscores the role of $^{1}H-^{1}H$ spin-diffusion efficiency in propagating polarization in crystalline samples. Although ^{1}H spin-diffusion rate is reduced with increased deuteration, spin heat capacity of the ^{1}H spin bath is reduced as well, leading to better bulk polarization away from Boltzmann distribution. The considerably lower enhancement (ε = 3.3) observed for the fully protonated OTP crystal suggests that the radical-poor regions of the sample were largely unenhanced by DNP, meaning that low ^{1}H concentration is required for polarization to penetrate into the crystalline core. Importantly, we observed that DNP enhancement remains appreciable (ε = 35) for glassy OTP even in samples that are 100% protonated. This can be attributed to a more homogeneous distribution of radicals as observed by the EPR spectrum, which means less reliance on long-range $^{1}H-^{1}H$ spin diffusion to spread polarization.

Implications for DNP of Pharmaceutical Systems. In terms of preparing solvent-free, amorphous pharmaceutical samples, we note that our preparation of OTP glass samples emulates hot-melt extrusion.[50] During hot-melt extrusion, API, excipients, and polymer carriers are melted and mixed at elevated temperatures and pressures to achieve a homogeneously dispersed solid-solution. On the basis of the results of this work, one can prepare drug samples for DNP via hot-melt extrusion and in theory should obtain reasonable ε, provided the radical polarization agent survives the process. Experiments are pending to investigate this hypothesis. Beyond hot-melt extrusion, a number of techniques exist to prepare amorphous, homogeneously dispersed pharmaceutical samples, including spray-dry dispersions, electrospinning, and freeze-drying. All of these methods can potentially be used to effectively prepare DNP samples.

We have begun DNP studies involving pharmaceutical glass-forming materials, most notably the anti-inflammation drug indomethacin. As a proof of concept, we prepared an indomethacin glass from lyophilized indomethacin powder (>99%, Sigma-Aldrich) doped with 0.5 mol % bTtereph. The DNP enhanced ^{13}C CPMAS spectrum showed an ε of 14, as shown in Figure 7. Taking into account Boltzmann population difference from acquiring the data at 80 K relative to room temperature, we obtain an overall enhancement, $\varepsilon^{\dagger}$ = 49, which corresponds to a savings of >2000-fold in acquisition time. The room temperature spectra of crystalline and amorphous indomethacin obtained at 11.74 T (Figure S7, Supporting Information) reveal that the resolution of multiple sites in the DNP enhanced spectrum is hampered as a result of acquisition at a relatively low field (5 T) and the fact that the majority of the drug comprises aromatic resonances confined in a narrow chemical-shift region. Higher field DNP spectrometers at 400 MHz (Bruker),[51] 600 MHz,[52] or at 700 MHz (FBML, MIT)[53] are expected to provide improved resolution. The combination of good DNP enhancement and good resolution will allow for more 2D solid-state NMR experiments in pharmaceutical

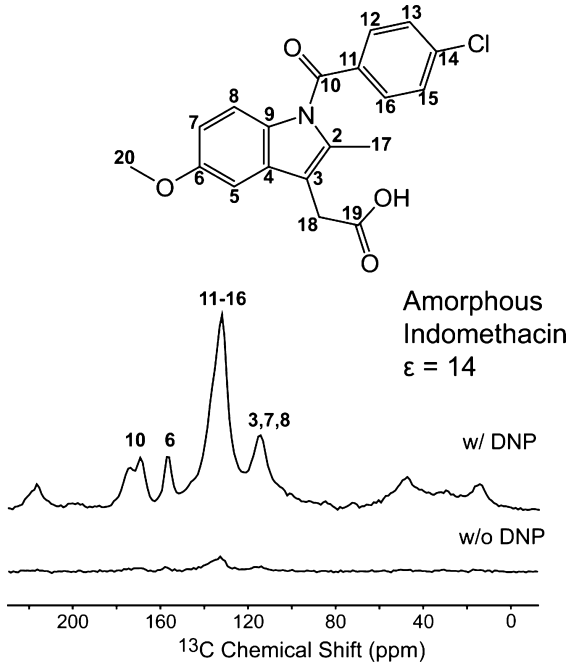

Figure 7. ^{13}C CPMAS DNP enhanced spectra of indomethacin glass doped with 0.5 mol % bTtereph.

research. Currently, 2D solid-state NMR experiments are not widely applied in pharmaceutical research because they are considered prohibitively time-consuming. However, recent experiements have shown that they can be valuable methods to analyze solid dispersion, particularly $^{1}H-^{13}C$ CP-HETCOR.[54−56] Successful application of DNP will make these 2D experiments more practical.

For DNP of crystalline pharmaceutical samples, we face two challenges: (1) the inhomogeneous distribution (clustering) of radical polarization agents during the crystallization process and (2) bulk isotope labeling of samples (i.e., synthesizing samples that are 95% deuterated) is not a common pharmaceutical practice. Moreover, deuteration of samples impacts CPMAS efficiency, so absolute signal sensitivity would be attenuated. To address the challenge of radical clustering, one can prepare a homogeneous mixture of samples and radicals as a suspension of protonated nanocrystals or microcrystals in a radical-containing solvent matrix. As observed by van der Wel et al., the small domain size of the nanocrystals (100−200 nm) results in an ε that is only slightly reduced relative to the glassy matrix.[57] Nanocrystals and nanoparticles with domain sizes less than 100 nm are found in pharmaceutical formulations.[58] To preserve the drug's solid-state structural and physical characteristics, the dispersant of choice should not dissolve the compound of interest. Recently, Rossini et al. demonstrated the idea in microcrystals by suspending glucose and sulfathiazole with domain sizes up to 500 μm in low ^{1}H density organic solvents such as 1,1,2,2-tetrabromoethane and 1,3-dibromobutane.[59] Takahashi et al. made the interesting observation that simply moisturizing the crystals appear to help DNP enhancement.[60] In their experiment using TOTAPOL-coated crystalline cellulose with domain size of 20 μm, ε of 2.4 was obtained in completely dried cellulose. However, when the cellulose was moisturized with a small amount of D_2O, ε increased to 20. Since TOTAPOL is soluble in water, the finding suggests that even a small amount of solvent seems to

dx.doi.org/10.1021/jp311237d | J. Phys. Chem. B 2013, 117, 3040−3046

alleviate the problem of radical clustering and thereby improves DNP performance.

CONCLUSIONS

DNP experiments of amorphous and crystalline OTP were compared to evaluate the feasibility of solvent-free DNP for pharmaceutical samples. We found that, due to superior distribution of radical polarization agents, OTP in the amorphous state consistently produced higher DNP enhancements than in the crystalline state. Considering that a variety of techniques exists to prepare amorphous, homogeneous pharmaceutical samples, such as hot-melt extrusion, electrospinning, and spray-dry dispersion, we propose that DNP can be used in combination with these methods to improve signal-to-noise of solid-state NMR experiments.

The effectiveness of DNP of crystalline systems is hindered by clustering of radical polarization agents leading to the creation of either radical-rich or -poor regions within the sample. This leads to longer polarization buildup times and smaller enhancements. However, crystalline samples maintain resolution due to their long-range order within the sample, whereas the distribution of sites (both angle and bond length variance) in amorphous solids cause inhomogeneous broadening, which will require higher fields and multiple dimension experiments for further structural information. It is important to note that this is an issue intrinsic to NMR regardless of DNP. NMR can probe amorphous, locally disordered structures that are not possible using traditional solid-state techniques such as diffraction methods. Coupling DNP with solid-state NMR now provides a faster method for obtaining structural information about disordered solids.

ASSOCIATED CONTENT

Supporting Information

Synthesis of bTtereph, TGA and DSC plots, DNP enhancement field profile, EPR profiles, EPR simulation, and additional NMR spectra. This material is available free of charge via the Internet at http://pubs.acs.org.

AUTHOR INFORMATION

Corresponding Author

*E-mail: rgg@mit.edu.

Author Contributions

The manuscript was written through contributions of all authors.

Notes

The authors declare the following competing financial interest(s): J. Walish owns and operates DyNuPol Inc., a supplier of polarization agents for dynamic nuclear polarization. The rest of the authors declare no competing financial interest.

ACKNOWLEDGMENTS

We thank Jeff Bryant, Blair Brettmann, Matthew Kiesewetter, and Eugene Cheung for useful discussions. We acknowledge the National Institute of Health for funding support of DNP projects at the Francis Bitter Magnet Laboratory (EB002804 and EB002026) and a grant to T.M.S., GM095843. V.K.M. is grateful to the Natural Sciences and Engineering Research Council of Canada for a postdoctoral fellowship. B.C. was partially supported by the Deutsche Forschungsgemeinschaft (Research Fellowship CO802/1-1).

REFERENCES

(1) Gibson, M. *Pharmaceutical Preformulation and Formulation: A Practical Guide from Candidate Drug Selection to Commercial Dosage Form*; CRC Press: Boca Raton, FL, 2001.
(2) Haleblian, J.; McCrone, W. *J. Pharm. Sci.* **1969**, *58* (8), 911−929.
(3) Rodriguez-Spong, B.; Price, C. P.; Jayasankar, A.; Matzger, A. J.; Rodriguez-Hornedo, N. *Adv. Drug Delivery Rev.* **2004**, *56* (3), 241−274.
(4) Geppi, M.; Mollica, G.; Borsacchi, S.; Veracini, C. A. *Appl. Spectrosc. Rev.* **2008**, *43* (3), 202−302.
(5) Yu, L.; Reutzel, S. M.; Stephenson, G. A. *Pharm. Sci. Technol. Today* **1998**, *1* (3), 118−127.
(6) Overhauser, A. W. *Phys. Rev.* **1953**, *92* (2), 411−415.
(7) Carver, T. R.; Slichter, C. P. *Phys. Rev.* **1953**, *92* (1), 212−213.
(8) Abragam, A.; Goldman, M. *Nuclear Magnetism: Order and Disorder*; Oxford University Press: Oxford, U.K., 1982.
(9) Wind, R. A.; Duijvestijn, M. J.; Vanderlugt, C.; Manenschijn, A.; Vriend, J. *Prog. Nucl. Magn. Reson. Spectrosc.* **1985**, *17*, 33−67.
(10) Singel, D. J.; Seidel, H.; Kendrick, R. D.; Yannoni, C. S. *J. Magn. Reson.* **1989**, *81* (1), 145−161.
(11) Afeworki, M.; Mckay, R. A.; Schaefer, J. *Macromolecules* **1992**, *25* (16), 4084−4091.
(12) Gerfen, G. J.; Becerra, L. R.; Hall, D. A.; Griffin, R. G.; Temkin, R. J.; Singel, D. J. *J. Chem. Phys.* **1995**, *102* (24), 9494−9497.
(13) Rosay, M.; Weis, V.; Kreischer, K. E.; Temkin, R. J.; Griffin, R. G. *J. Am. Chem. Soc.* **2002**, *124* (13), 3214−3215.
(14) Ardenkjaer-Larsen, J. H.; Fridlund, B.; Gram, A.; Hansson, G.; Hansson, L.; Lerche, M. H.; Servin, R.; Thaning, M.; Golman, K. *Proc. Natl. Acad. Sci. U.S.A.* **2003**, *100* (18), 10158−10163.
(15) Mak-Jurkauskas, M. L.; Bajaj, V. S.; Hornstein, M. K.; Belenky, M.; Griffin, R. G.; Herzfeld, J. *Proc. Natl. Acad. Sci. U.S.A.* **2008**, *105* (3), 883−888.
(16) Bajaj, V. S.; Mak-Jurkauskas, M. L.; Belenky, M.; Herzfeld, J.; Griffin, R. G. *Proc. Natl. Acad. Sci. U.S.A.* **2009**, *106* (23), 9244−9249.
(17) Debelouchina, G. T.; Bayro, M. J.; van der Wel, P. C. A.; Caporini, M. A.; Barnes, A. B.; Rosay, M.; Maas, W. E.; Griffin, R. G. *Phys. Chem. Chem. Phys.* **2010**, *12* (22), 5911−5919.
(18) Lumata, L.; Merritt, M. E.; Hashami, Z.; Ratnakar, S. J.; Kovacs, Z. *Angew. Chem., Int. Ed.* **2012**, *51* (2), 525−527.
(19) Lesage, A.; Lelli, M.; Gajan, D.; Caporini, M. A.; Vitzthum, V.; Mieville, P.; Alauzun, J.; Roussey, A.; Thieuleux, C.; Mehdi, A.; et al. *J. Am. Chem. Soc.* **2010**, *132* (44), 15459−15461.
(20) Albers, M. J.; Bok, R.; Chen, A. P.; Cunningham, C. H.; Zierhut, M. L.; Zhang, V. Y.; Kohler, S. J.; Tropp, J.; Hurd, R. E.; Yen, Y. F.; et al. *Cancer Res.* **2008**, *68* (20), 8607−8615.
(21) Keshari, K. R.; Kurhanewicz, J.; Bok, R.; Larson, P. E. Z.; Vigneron, D. B.; Wilson, D. M. *Proc. Natl. Acad. Sci. U.S.A.* **2011**, *108* (46), 18606−18611.
(22) Kurhanewicz, J.; Vigneron, D. B.; Brindle, K.; Chekmenev, E. Y.; Comment, A.; Cunningham, C. H.; DeBerardinis, R. J.; Green, G. G.; Leach, M. O.; Rajan, S. S.; et al. *Neoplasia* **2011**, *13* (2), 81−97.
(23) Hall, D. A.; Maus, D. C.; Gerfen, G. J.; Inati, S. J.; Becerra, L. R.; Dahlquist, F. W.; Griffin, R. G. *Science* **1997**, *276* (5314), 930−932.
(24) Barnes, A. B.; Corzilius, B.; Mak-Jurkauskas, M. L.; Andreas, L. B.; Bajaj, V. S.; Matsuki, Y.; Belenky, M. L.; Lugtenburg, J.; Sirigiri, J. R.; Temkin, R. J.; et al. *Phys. Chem. Chem. Phys.* **2010**, *12* (22), 5861−5867.
(25) Barnes, A. B.; De Paepe, G.; van der Wel, P. C. A.; Hu, K. N.; Joo, C. G.; Bajaj, V. S.; Mak-Jurkauskas, M. L.; Sirigiri, J. R.; Herzfeld, J.; Temkin, R. J.; et al. *Appl. Magn. Reson.* **2008**, *34* (3−4), 237−263.
(26) Lumata, L.; Jindal, A. K.; Merritt, M. E.; Malloy, C. R.; Sherry, A. D.; Kovacs, Z. *J. Am. Chem. Soc.* **2011**, *133* (22), 8673−8680.
(27) Matsuki, Y.; Maly, T.; Ouari, O.; Karoui, H.; Le Moigne, F.; Rizzato, E.; Lyubenova, S.; Herzfeld, J.; Prisner, T.; Tordo, P.; et al. *Angew. Chem., Int. Ed.* **2009**, *48* (27), 4996−5000.
(28) Vitzthum, V.; Borcard, F.; Jannin, S.; Morin, M.; Mieville, P.; Caporini, M. A.; Sienkiewicz, A.; Gerber-Lemaire, S.; Bodenhausen, G. *ChemPhysChem* **2011**, *12* (16), 2929−2932.

(29) Lilly Thankamony, A.; Lafon, O.; Lu, X.; Aussenac, F.; Rosay, M.; Trébosc, J.; Vezin, H.; Amoureux, J.-P. *Appl. Magn. Reson.* **2012**, *43* (1), 237−250.
(30) Tolle, A. *Rep. Prog. Phys.* **2001**, *64* (11), 1473−1532.
(31) Andrews, J. N.; Ubbelohde, A. R. *Proc. R. Soc. A* **1955**, *228* (1175), 435−447.
(32) Becerra, L. R.; Gerfen, G. J.; Temkin, R. J.; Singel, D. J.; Griffin, R. G. *Phys. Rev. Lett.* **1993**, *71* (21), 3561−3564.
(33) Barnes, A. B.; Mak-Jurkauskas, M. L.; Matsuki, Y.; Bajaj, V. S.; van der Wel, P. C. A.; DeRocher, R.; Bryant, J.; Sirigiri, J. R.; Temkin, R. J.; Lugtenburg, J.; et al. *J. Magn. Reson.* **2009**, *198* (2), 261−270.
(34) Bennett, A. E.; Rienstra, C. M.; Auger, M.; Lakshmi, K. V.; Griffin, R. G. *J. Chem. Phys.* **1995**, *103* (16), 6951−6958.
(35) Pines, A.; Waugh, J. S.; Gibby, M. G. *J. Chem. Phys.* **1972**, *56* (4), 1776−1777.
(36) Rosay, M. M. *Sensitivity-Enhanced Nuclear Magnetic Resonance of Biological Solids*; Massachusetts Institute of Technology: Cambridge, MA, 2001.
(37) Kagawa, A.; Murokawa, Y.; Takeda, K.; Kitagawa, M. *J. Magn. Reson.* **2009**, *197* (1), 9−13.
(38) Akbey, U.; Franks, W. T.; Linden, A.; Lange, S.; Griffin, R. G.; van Rossum, B. J.; Oschkinat, H. *Angew. Chem., Int. Ed.* **2010**, *49* (42), 7803−7806.
(39) Corzilius, B.; Smith, A. A.; Griffin, R. G. *J. Chem. Phys.* **2012**, *137* (5), 054201.
(40) Hu, K. N.; Yu, H. H.; Swager, T. M.; Griffin, R. G. *J. Am. Chem. Soc.* **2004**, *126* (35), 10844−10845.
(41) Kessenikh, A. V.; Manenkov, A. A. *Sov. Phys.—Solid State* **1963**, *5* (4), 835−837.
(42) Hwang, C. F.; Hill, D. A. *Phys. Rev. Lett.* **1967**, *18* (4), 110−.
(43) Hwang, C. F.; Hill, D. A. *Phys. Rev. Lett.* **1967**, *19* (18), 1011.
(44) Wollan, D. S. *Phys. Rev. B* **1976**, *13* (9), 3671−3685.
(45) Wollan, D. S. *Phys. Rev. B* **1976**, *13* (9), 3686−3696.
(46) Song, C. S.; Hu, K. N.; Joo, C. G.; Swager, T. M.; Griffin, R. G. *J. Am. Chem. Soc.* **2006**, *128* (35), 11385−11390.
(47) Maly, T.; Cui, D.; Griffin, R. G.; Miller, A. F. *J. Phys. Chem. B* **2012**, *116* (24), 7055−65.
(48) Stoll, S.; Schweiger, A. *J. Magn. Reson.* **2006**, *178* (1), 42−55.
(49) Dementyev, A. E.; Cory, D. G.; Ramanathan, C. *Phys. Rev. Lett.* **2008**, *100*, 12.
(50) Breitenbach, J. *Eur. J. Pharm. Biopharm.* **2002**, *54* (2), 107−117.
(51) Rosay, M.; Tometich, L.; Pawsey, S.; Bader, R.; Schauwecker, R.; Blank, M.; Borchard, P. M.; Cauffman, S. R.; Felch, K. L.; Weber, R. T.; et al. *Phys. Chem. Chem. Phys.* **2010**, *12* (22), 5850−5860.
(52) Matsuki, Y.; Takahashi, H.; Ueda, K.; Idehara, T.; Ogawa, I.; Toda, M.; Akutsu, H.; Fujiwara, T. *Phys. Chem. Chem. Phys.* **2010**, *12* (22), 5799−5803.
(53) Barnes, A. B.; Markhasin, E.; Daviso, E.; Michaelis, V. K.; Nanni, E. A.; Jawla, S. K.; Mena, E. L.; DeRocher, R.; Thakkar, A.; Woskov, P. P.; et al. *J. Magn. Reson.* **2012**, *224* (0), 1−7.
(54) Geppi, M.; Guccione, S.; Mollica, G.; Pignatello, R.; Veracini, C. A. *Pharm. Res.* **2005**, *22* (9), 1544−1555.
(55) Mollica, G.; Geppi, M.; Pignatello, R.; Veracini, C. A. *Pharm. Res.* **2006**, *23* (9), 2129−2140.
(56) Pham, T. N.; Watson, S. A.; Edwards, A. J.; Chavda, M.; Clawson, J. S.; Strohmeier, M.; Vogt, F. G. *Mol. Pharmaceutics* **2010**, *7* (5), 1667−1691.
(57) van der Wel, P. C. A.; Hu, K. N.; Lewandowski, J.; Griffin, R. G. *J. Am. Chem. Soc.* **2006**, *128* (33), 10840−10846.
(58) Kipp, J. E. *Int. J. Pharm.* **2004**, *284* (1−2), 109−122.
(59) Rossini, A. J.; Zagdoun, A.; Hegner, F.; Schwarzwalder, M.; Gajan, D.; Coperet, C.; Lesage, A.; Emsley, L. *J. Am. Chem. Soc.* **2012**, *134* (40), 16899−16908.
(60) Takahashi, H.; Lee, D.; Dubois, L.; Bardet, M.; Hediger, S.; De Paepe, G. *Angew. Chem., Int. Ed.* **2012**, *51* (47), 11766−11769.